Analogs of 3-Hydroxy-1*H*-1-benzazepine-2,5-dione: Structure−Activity Relationship at *N*-Methyl-D-aspartate Receptor Glycine Sites

Anthony P. Guzikowski,[†] Sui Xiong Cai,[‡] Stephen A. Espitia,[‡] Jon E. Hawkinson,[‡] James E. Huettner,[§] Daniel F. Nogales,[†] Minhtam Tran,[‡] Richard M. Woodward,[‡] Eckard Weber,*[,‡] and John F. W. Keana*[,†]

CoCensys, Inc., 213 Technology Drive, Irvine, California 92618, Department of Cell Biology and Physiology, Washington University School of Medicine, St. Louis, Missouri 63110, and Department of Chemistry, University of Oregon, Eugene, Oregon 97403

Received July 3, 1996[⊗]

A series of aromatic and azepine ring-modified analogs of 3-hydroxy-1*H*-1-benzazepine-2,5-dione (HBAD) were synthesized and evaluated as antagonists at NMDA receptor glycine sites. Aromatic ring-modified HBADs were generally prepared via a Schmidt reaction with substituted 2-methoxynaphthalene-1,4-diones followed by demethylation. Electrophilic aromatic substitution of benzazepine 3-methyl ethers gave 7-substituted analogs. The preparation of multiply substituted 2-methoxynaphthalene-1,4-diones was effected via Diels−Alder methodology utilizing substituted butadienes with 2-methoxybenzoquinones followed by aromatization. Structural modifications, such as elimination of the aromatic ring, removal of the 3-hydroxyl group, and transfer of the hydroxyl group from C-3 to C-4, were also studied. An initial evaluation of NMDA antagonism was performed using a [^{3}H]MK801 binding assay. HBADs demonstrating NMDA antagonist activity as indicated by inhibition of [^{3}H]MK801 binding were further evaluated employing a [^{3}H]-5,7-dichlorokynurenic acid (DCKA) glycine site binding assay. Selected HBADs were characterized for functional antagonism of NMDA and AMPA receptors using electrophysiological assays in *Xenopus* oocytes and cultured rat cortical neurons. Antagonist potency of HBADs showed good correlation between the different assay systems. HBADs substituted at the 8-position possessed the highest potency with the 8-methyl (**5**), 8-chloro (**6**), and 8-bromo (**7**) analogs being the most active. For HBAD **6**, the IC_{50} in [^{3}H]-DCKA binding assays was 0.013 μM and the K_b values for antagonism of NMDA receptors in oocytes (NR1a/2C) and cortical neurons were 0.026 and 0.048 μM, respectively. HBADs also antagonized AMPA-preferring non-NMDA receptors expressed in oocytes but at a lower potency than corresponding inhibition of NMDA receptors. HBADs demonstrating a high potency for NMDA glycine sites showed the highest steady-state selectivity index relative to AMPA receptors. Substitution at the 6-, 7-, and 9-positions generally reduced or eliminated glycine site affinity. Moving the hydroxyl group from C-3 to C-4 reduced receptor affinity, and potency was eliminated by the removal of the aromatic ring or the hydroxyl group. These data indicate that the HBAD series has specific structural requirements for high receptor affinity. With the exception of substitution at C-8, modified HBADs generally have a lower affinity at NMDA receptor glycine sites than the parent compound **3**. Mouse maximum electroshock-induced seizure studies show that the three HBADs selected for testing have *in vivo* potency with the 6,8-dimethyl analog (**52**) being the most potent (ED_{50} = 3.9 mg/kg, iv).

Introduction

N-Methyl-D-aspartate (NMDA), kainate, and α-amino-3-hydroxy-5-methylisoxazole-4-propionic acid (AMPA) receptors are the three major types of ionotropic excitatory amino acid receptors found in the mammalian central nervous system.[1] The NMDA receptor in particular has been associated with a variety of acute and chronic neurological disorders including the brain damage resulting from stroke, epilepsy, Alzheimer's disease, and AIDS-related dementia.[2] Receptor overstimulation, caused by excessive glutamate in the synaptic region, is believed to contribute to the symptomatology of these disorders. The overstimulation leads to pathological levels of intracellular Ca^{2+} triggering a cascade of events leading to neuronal death.[3] In addition to glutamate, the amino acid glycine is a necessary coagonist for activation of NMDA receptors.[4] Therefore, compounds such as 3′-(3-thienyloxy)-3-phenyl-4-hydroxy-1*H*-quinolin-2-one (**1**),[5] ACEA 1021 (**2**),[6] and 8-chloro-3-hydroxy-1*H*-1-benzazepine-2,5-dione (**6**),[7] which act as antagonists at NMDA receptor glycine sites, may offer a means for the treatment of neurodegenerative disorders associated with excitotoxicity.[8]

Our interest in the 3-hydroxy-1*H*-1-benzazepine-2,5-dione (HBAD) series arose from a report that described NMDA receptor glycine site antagonism by HBADs **3**−**5**, with **5** possessing submicromolar potency.[9] Subsequently, the synthesis of **6**−**8** and several other halo-substituted HBADs was described in the patent literature,[7] but the pharmacological characterization of these compounds was very limited. In order to establish a more detailed structure−activity relationship (SAR), a series of structurally modified HBADs was synthesized. NMDA antagonist activity was determined initially by glycine dependent inhibition of [^{3}H]MK801 binding. Affinity at NMDA receptor glycine sites was determined for the active compounds using a [^{3}H]-5,7-dichloro-

* Authors to whom correspondence should be addressed.
† University of Oregon.
‡ CoCensys, Inc.
§ Washington University School of Medicine.
⊗ Abstract published in *Advance ACS Abstracts,* October 1, 1996.

S0022-2623(96)00479-7 CCC: $12.00

Scheme 1[a]

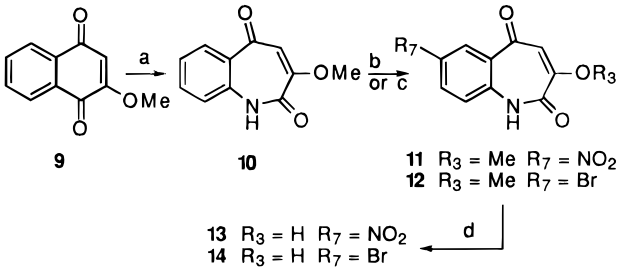

[a] (a) NaN_3, H_2SO_4; (b) KNO_3, H_2SO_4; (c) NBS, H_2SO_4; (d) H_2SO_4, H_2O/EtOH, Δ.

kynurenic acid (DCKA) assay. Functional antagonism of NMDA and AMPA receptors was determined using electrophysiological assays. *In vivo* potency was measured using a mouse maximum electroshock-induced seizure (MES) model.

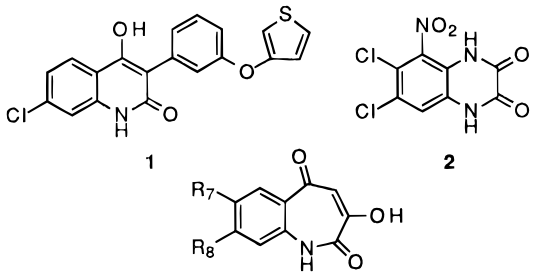

Chemistry

Aromatic Ring-Substituted HBADs. Aromatic ring-modified HBADs were generally synthesized via a Schmidt reaction of appropriate 2-methoxynaphthlene-1,4-diones as described by Birchall and Rees[10] with subsequent modifications described by Chapdelaine and McLaren[7] followed by demethylation by either aqueous acid hydrolysis or with BBr_3 in CH_2Cl_2. HBADs **3** and **5**−**8** were prepared as previously reported.[7,9,10]

The 7-substituted HBADs **13** and **14** were obtained by direct electrophilic nitration or bromination of **10** (formed *in situ* by a Schmidt reaction on **9**[11]) followed by hydrolysis of the intermediate methyl ethers **11** and **12** (Scheme 1). The regiochemistry of the Schmidt reaction and of the nitration reaction was confirmed by single-crystal X-ray analysis of **11**. The regiochemistry of the bromination reaction was assigned by analogy with the nitration reaction and by NMR comparison of **14** with **7**.

Catalytic hydrogenation of **11** employing a quinoline-poisoned catalyst to inhibit reduction of the 3,4-double bond gave amine **15** (Scheme 2). Derivatizations of the amino group of **15** gave the methyl ethers **16**−**18**. Aqueous acid hydrolysis gave HBADs **19**−**21**.

The synthesis of multiply substituted HBADs employed Diels−Alder methodology for the preparation of the requisite intermediate 2-methoxynaphthalene-1,4-diones (Scheme 3).[12] Allowing methyl-substituted butadienes **22**−**25** to react with **26**[13] yielded the corresponding crude adducts (not shown). The reactions of dienes **22** and **23** were approximately 90% regioselective as determined by ^1H NMR. Bohlman et al.[12] reported that the major regioisomer obtained from the reaction of **22**

Scheme 2[a]

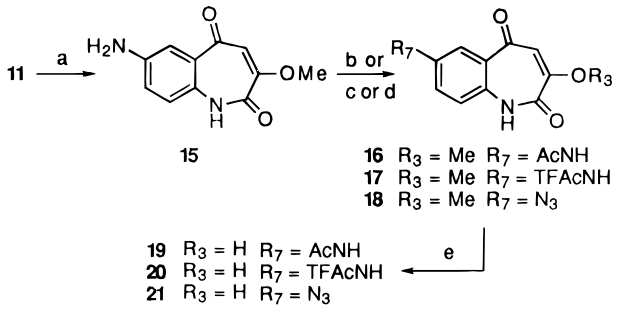

[a] (a) H_2, quinoline, MeOH/CH_2Cl_2; (b) Ac_2O, MeOH/CH_2Cl_2; (c) TFAA, EtOAc; (d) $NaNO_2$, HCl, H_2O then NaN_3; (e) H_2SO_4, H_2O/EtOH, Δ.

Scheme 3[a]

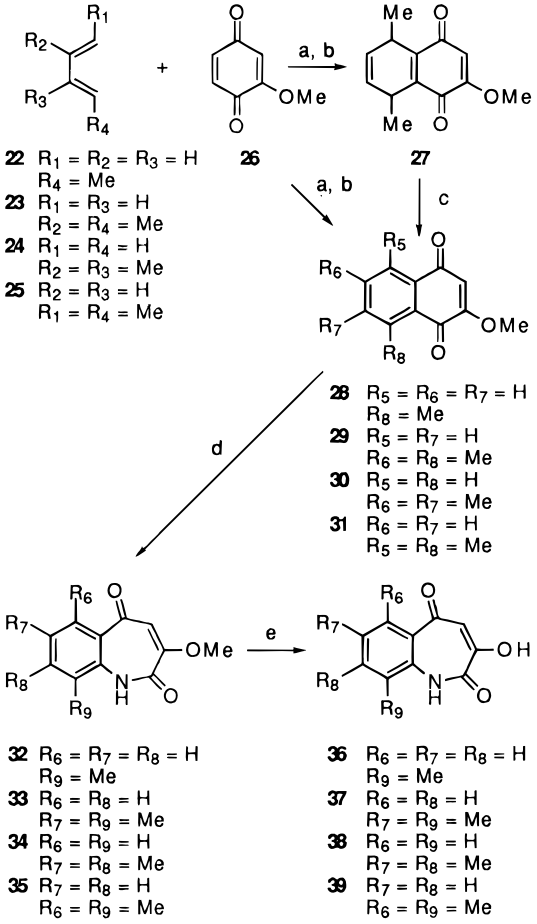

[a] (a) Toluene, hydroquinone, Δ; (b) O_2, Et_3N, MeOH; (c) DDQ, toluene, Δ; (d) NaN_3, H_2SO_4 or CF_3SO_3H; (e) BBr_3, CH_2Cl_2.

with **26** had the methyl group in the 8-position of the hydronaphthalene ring system. The regiochemical assignment for the major product of this reaction was tentatively based on this report. Confirmation of this assignment was made by single-crystal X-ray analysis of the corresponding HBAD (*vide infra*). The regiochemical assignment for the major adduct derived from **23** was based on analogy with the reaction of **22**. The crude adducts derived from **22**−**24** were directly converted into quinone derivatives **28**−**30**,[12,14] respectively, via a base-catalyzed oxidation followed by purification. In the case of the adduct derived from **25**, this oxidation stopped at the 5,8-dihydronaphthalene-1,4-dione **27**. Treatment of **27** with DDQ in refluxing toluene gave the desired **31**. Quinones **28**−**31** were carried on to the

Table 1. Physical Data, NMR Spectroscopic Data, and Methods of Preparation for Substituted HBADs

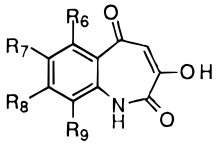

compd no.	R_6	R_7	R_8	R_9	method/ yield (%)[a]	mp (°C)	formula[b]	^{1}H NMR[c]
13	H	NO_2	H	H	A/58	250 dec[d]	$C_{10}H_6N_2O_5$	6.45, 7.61 (d, J = 9.0), 8.39 (dd, J = 9.0, 2.7), 8.79 (d, J = 2.7), 11.14 (b), 12.04
14	H	Br	H	H	A/46	284−286 dec	$C_{10}H_6BrNO_3 \cdot 0.16H_2O$	6.42, 7.41 (d, J = 9.0), 7.80 (dd, J = 8.7, 2.4), 8.10 (d, J = 2.1), 10.86 (b), 11.71
19	H	AcNH	H	H	A/70	310 dec[d]	$C_{12}H_{10}N_2O_4 \cdot 0.40H_2O$	2.03 (3H), 6.41, 7.39 (d, J = 8.7), 7.86 (dd, J = 8.7, 2.1), 8.20 (d, J = 1.8), 10.15, 10.60 (b), 11.59
20	H	TFAcNH	H	H	A/74	330 dec[d]	$C_{12}H_7F_3N_2O_4 \cdot 0.20H_2O$	6.43, 7.49 (d, J = 8.7), 7.90 (dd, J = 8.7, 2.1), 8.36 (d, J = 2.1), 10.73 (b), 11.45, 11.69
21	H	N_3	H	H	A/18[e]	190 dec[d]	$C_{10}H_6N_4O_3$	6.42, 7.39 (dd, J = 8.7, 2.7). 7.51 (d, J = 8.7), 7.66 (d, J = 2.7), 10.78 (b), 11.70
36	H	H	H	Me	B/52	184−186 dec	$C_{11}H_9NO_3 \cdot 0.50H_2O$	2.46 (3H), 6.28, 7.19 (t, J = 7.5), 7.48 (d, J = 7.2), 7.67 (d, J = 7.8), 9.94, 10.85 (b)
37	H	Me	H	Me	B/69	211−213 dec	$C_{12}H_{11}NO_3$	2.28 (3H), 2.42 (3H), 6.27, 7.31, 7.47, 9.90, 10.74 (b)
38	H	Me	Me	H	B/77	302−304 dec[f]	$C_{12}H_{11}NO_3$	2.23 (3H), 2.24 (3H), 6.39, 7.24, 7.80, 10.46, 11.49
39	Me	H	H	Me	B/12	183−185 dec	$C_{12}H_{11}NO_3$	2.24 (3H), 2.35 (3H), 6.20, 7.03 (d, J = 7.8), 7.25 (d, J = 7.8), 9.98, 10.53 (b)
51	Me	H	H	H	B/45	188−189 dec	$C_{11}H_9NO_3$	2.34 (3H), 6.30, 7.09 (d, J = 7.2), 7.21 (d, J = 8.1), 7.37 (t, J = 7.8), 10.39, 11.20
52	Me	H	Me	H	B/49	189−191 dec	$C_{12}H_{11}NO_3$	2.26 (3H), 2.31 (3H), 6.28, 6.92, 7.01, 10.29, 11.12
53	Me	Me	H	H	B/55	206−208 dec	$C_{12}H_{11}NO_3$	2.16 (3H), 2.23 (3H), 6.30, 7.09 (d, J = 8.1), 7.28 (d, J = 8.4), 10.31 (b), 11.08
55	Me	NO_2	Me	H	B/43	230−231 dec	$C_{12}H_{10}N_2O_5$	2.17 (3H), 2.23 (3H), 6.34, 7.23, 10.72, 11.40
60	H	H	Et	H	*g*	250−251 dec	$C_{12}H_{11}NO_3$	1.18 (t, J = 7.5, 3H), 2.64 (q, J = 7.5, 2H), 6.40, 7.13 (d, J = 8.4), 7.31, 7.97 (d, J = 8.1), 10.51, 11.51

[a] For detailed methods, see the Experimental Section. Method A is H_2SO_4 in H_2O/EtOH, Δ. Method B is BBr_3 in CH_2Cl_2 at 25 °C. [b] Analyses for C, H, and N are within ±0.40% of theoretical values. [c] Unless otherwise noted, values listed are for one-proton singlets. Abbreviations: b = broad singlet, d = doublet, dd = doublet doublet, t = triplet, q = quartet, and m = multiplet. Splitting values are reported in hertz (Hz). [d] Decomposition without melting. [e] Total yield for the reaction sequences starting from **15**. [f] Lit. mp 288 °C dec; ref 10. [g] HBAD **60** was generously supplied by Prof. Alun H. Rees and prepared according to the procedures detailed in ref 10.

benzazepine methyl ethers **32**−**35** as described above. Demethylation employing BBr_3 in CH_2Cl_2 gave HBADs **36**−**39**. The structure of **36** was established by single-crystal X-ray analysis thus confirming the regioselectivity of the Schmidt reaction of **28** and of the reported Diels−Alder reaction of **22** with **26**.[12]

The regiochemical assignments of HBAD **37** and its precursor **29** were based on the ^{1}H NMR comparison of methyl ether **33** with methyl ethers **32**, **34**, and **35**. Chemical shift values for the amide proton of methyl ethers **32** and **35**, where a *peri*-methyl group is present, are δ 9.45 and 9.96, respectively. Conversely, the chemical shift of the amide proton of methyl ether **34**, which does not have a *peri*-methyl group, is δ 11.19. The chemical shift of the amide proton of methyl ether **33** is δ 9.90, thus providing confirmation for the regiochemical assignments.

In order to prepare HBADs analogous to **36** and **37** but with the opposite regiochemistry in the aromatic ring portion, the regioselectivity of the Diels−Alder reaction required alteration. Tegmo-Larsson et al.[15] reported that 2,5-dimethoxybenzoquinone underwent a Diels−Alder reaction with **22** to give an adduct which, upon loss of MeOH, gave the 5,8-dihydronaphthalene with the methyl group in the desired 5-position. In our hands, this reaction proceeded slowly and was impractical for our needs. Therefore, we investigated the Diels−Alder reaction of 2-bromo-5-methoxybenzoquinone (**42**)[16] with a series of 1,3-dienes (Scheme 4). Dienophile **42** was prepared by the bromination of hydroquinone **40**[17] followed by periodate oxidation of bromohydroquinone **41**. The adduct (not shown) derived from the reaction of **22** with **42** formed readily but turned to a black tar upon isolation. Therefore, this adduct and the adducts derived from **23** and **45** were not isolated but immediately treated with Et_3N to yield the corresponding 5,8-dihydronaphthalene-1,4-diones (not shown) by dehydrobromination. Subsequent oxidation with MnO_2 in refluxing $CHCl_3$ yielded **43**, **44**, and a mixture of **46** and **47**, respectively. Compounds **43** and **44** were regiochemically pure by ^{1}H NMR. The regiochemistry of these compounds was assigned by NMR comparison with **28** and **29**. Quinones **46** and **47** were obtained as a 3:7 mixture (by NMR), respectively. Isolation of **47** was effected by crystallization, and the regiochemistry was tentatively based on analogy with **43** and **44**. Conversion of **43**, **44**, and **47** to HBADs **51**−**53** was performed as described above.

The regiochemistry of **50**, and thus that of **47** and **53**, was confirmed by ^{1}H NMR analysis. The chemical shift value for the amide proton of **50** (δ 10.88) is consistent with the values measured for the amide protons of **48** and **49** (δ 11.00 and 10.94, respectively) and inconsistent with values measured for HBAD methyl ethers that

Scheme 4[a]

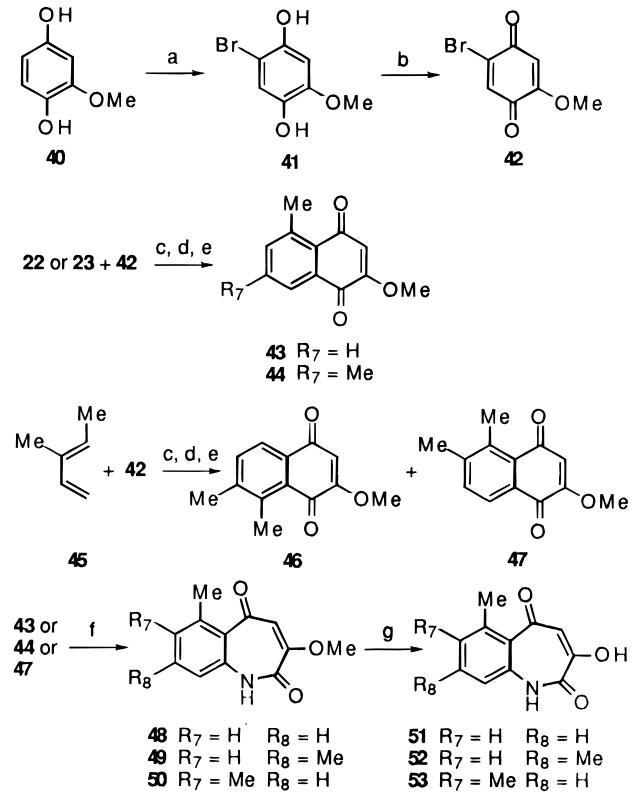

[a] (a) Br_2, AcOH; (b) $NaIO_4$, $H_2O/CHCl_3$; (c) toluene, Δ; (d) Et_3N, toluene/MeOH; (e) MnO_2, $CHCl_3$, Δ; (f) NaN_3, H_2SO_4; (g) BBr_3, CH_2Cl_2.

Scheme 5[a]

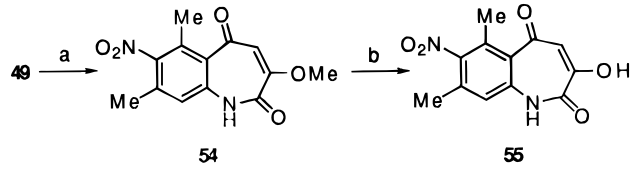

[a] KNO_3, H_2SO_4; (b)BBr_3, CH_2Cl_2.

possess a *peri*-methyl group (*vide supra*). Also, irradiation of the amide proton of **50** gave the expected NOE enhancement (22%) of the H-9 doublet.

Nitration of **49** (formed *in situ* via a Schmidt reaction of **44**) gave the nitromethyl ether **54** (Scheme 5). Demethylation gave the 7-nitro HBAD **55**. The regiochemistry of the nitration reaction was assigned by analogy with the nitration of **10** and by a NOE experiment on **54**. Irradiation of the amide proton resulted in a 23% enhancement of the H-9 singlet.

Other Modified 1*H*-1-Benzazepine-2,5-diones. The syntheses of **56**−**58** were performed according to known literature procedures.[18−20] Oxime **59** was prepared by the reaction of **3** with $NaNO_2$ in aqueous base followed by treatment with H_2SO_4.

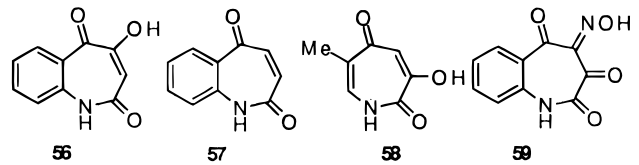

Radioligand Binding Studies

All HBADs were initially screened for NMDA antagonism by measuring inhibition of glycine dependent [^{3}H]-MK801 binding to rat brain cortical membranes by methods previously described.[21] HBADs inhibiting [^{3}H]-MK801 binding with an IC_{50} < 300 μM were considered to be potentially active as antagonists at NMDA receptors (Table 2). Active compounds were evaluated further using the selective glycine site ligand [^{3}H]DCKA.[22]

Table 2. Radioligand Binding Data at NMDA Receptors for HBAD Analogs

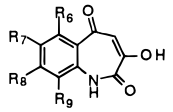

					IC_{50}(μM)[a]	
compd no.	R_6	R_7	R_8	R_9	[^{3}H]MK801	[^{3}H]DCKA
3	H	H	H	H		0.83 ± 0.06
5	H	H	Me	H		0.13 ± 0.01
6	H	H	Cl	H		0.013 ± 0.002
7	H	H	Br	H		0.079 ± 0.007
8	H	H	F	H		0.49 ± 0.03
13	H	NO_2	H	H		12 ± 2.1
14	H	Br	H	H	>300	
19	H	AcNH	H	H		>100
20	H	TFAcNH	H	H	>300	
21	H	N_3	H	H	>300	
36	H	H	H	Me	>300	
37	H	Me	H	Me	>300	
38	H	Me	Me	H		0.24 ± 0.05
39	Me	H	H	Me	>300	
51	Me	H	H	H		13 ± 0.9
52	Me	H	Me	H		0.30 ± 0.04
53	Me	Me	H	H	>300	
55	Me	NO_2	Me	H		2.2 ± 0.2
56						>100
57					>300	
58					>300	
59					>300	
60	H	H	Et	H		5.1 ± 0.8

[a] IC_{50} values are mean ± SEM and are the result of a minimum of three determinations.

Electrophysiology in *Xenopus* Oocytes

To confirm that HBADs are functional antagonists at NMDA receptors, seven compounds were assayed for inhibition of NMDA responses in *Xenopus* oocytes expressing the cloned rat NMDA receptor subunit combination NR1a/2C.[23−25] Potency of antagonism was assessed by determination of apparent antagonist dissociation constants (K_b values) calculated from partial (3−5 point) concentration−inhibition curves (Table 3).[23,26] Calculation of K_b values assumes that inhibition of membrane current responses is by competitive antagonism at glycine coagonist sites.

Like various other classes of glycine site antagonist, e.g., quinoxalinediones (QXs),[6] tetrahydroquinolin-3-

Table 3. Functional Antagonism of Rat Brain NMDA and AMPA Receptors by HBADs

compd no.	K_b (μM) NMDA (glycine)[a]	K_b (μM) AMPA (glutamate)[b]	K_b AMPA / K_b NMDA[c]	n[d]
		Oocyte Recordings		
3	1.3[e] (1.2−1.5)[f]	42 (39−46)	32	4, 3
5	0.25 (0.24−0.26)	9.9 (8.7−11)	40	3, 4
6	0.026 (0.025−0.028)	2.0 (1.7−2.3)	77	7, 5
7	0.026 (0.024−0.029)	2.7 (2.3−3.3)	100	4, 6
8	0.21 (0.18−0.24)	5.3 (4.8−5.8)	25	3, 4
38	0.086 (0.080−0.094)	3.8 (3.5−4.2)	44	4, 4
56	>55	>240		2, 2
		Neuron Recordings[g]		
3[h]	3.0[i] (2.7−3.4)	65[j] (53−80)	22	2, 2
5	0.47 (0.41−0.54)	6.4 (5.5−7.5)	14	3, 3
6	0.048 (0.038−0.061)	10 (9.2−11.7)	210	5, 8
7	0.061 (0.050−0.073)			6, −

[a] Inhibition of NMDA receptors was measured in oocytes expressing cloned rat brain receptor subunits (NR1a/2C).[24] Affinity of HBADs for glycine binding sites was estimated from inhibition of currents elicited by 1 μM glycine and 100 μM glutamate. [b] Inhibition of AMPA-preferring non-NMDA receptors was measured in oocytes expressing rat cerebral cortex poly(A)$^+$ RNA. Affinity of HBADs for AMPA receptors was estimated from inhibition of currents elicited by 10 μM AMPA. [c] Steady-state selectivity index was estimated by dividing K_b AMPA by K_b NMDA. [d] Number of cells examined for NMDA and AMPA, respectively. [e] K_b values given to two significant figures. [f] 95% confidence intervals adjusted to the linear scale. [g] Recordings were made using cultured rat cortical neurons. [h] Values taken from ref 9. [i] K_b values for glycine sites were estimated from the rightward displacement of glycine concentration−response curves by fixed concentrations of HBADs (NMDA = 0.1 or 1 mM). [j] K_b values for AMPA receptor glutamate sites were estimated from the displacement of concentration response curves for kainate.

oximes,[27] kynurenic acids (KAs),[28] etc., HBADs also antagonize AMPA-preferring non-NMDA receptors.[9] In the present study, antagonism of AMPA receptors was measured in oocytes expressing rat cerebral cortex poly-(A)$^+$ RNA.[23,29] As described for NMDA receptors, potency of inhibition was estimated from partial concentration−inhibition curves on currents elicited, in this case, by 10 μM AMPA (Table 3).

Electrophysiology in Mammalian Neurons

Effects of HBADs on neuronal NMDA and AMPA receptors were measured using whole cell recordings from cultured rat cortical neurons. Potency of HBADs **6** and **7** was estimated from the rightward displacement of steady-state agonist concentration−response curves.[9,23] Agonists were glycine for NMDA receptors and kainate for AMPA receptors.

Under control conditions the EC_{50} and slope values for activation of NMDA receptors by glycine were 0.18 μM and 1.1, respectively. Inhibition induced by HBADs **6** and **7** was associated with a rightward displacement of the glycine concentration−response curve and was fully surmountable when the glycine concentration was increased to 100 μM (Figure 1). K_b values calculated from the shift in apparent glycine affinity are given in Table 3. These experiments confirm that antagonism is predominantly due to competitive inhibition at glycine sites. Antagonism did, however, deviate from the strict competitive model ($F_{1,45} = 6.3$ for **6**, $F_{1,50} = 12$ for **7**). For both HBADs, deviation from the model was due to slightly increased slopes in the presence of drug.

Under control conditions, the EC_{50} and slope values for kainate as an agonist of AMPA receptors were 160 μM and 1.3, respectively. As described for glycine, inhibition of AMPA receptors by HBAD **6** was due to a rightward shift in the kainate concentration−response relationship (not illustrated). With 50 μM HBAD **6**, the EC_{50} for kainate was 930 μM and the slope was 1.2. In this case, inhibition conformed with the competitive model ($F_{1,96} = 0.65$). The K_b value calculated from this pair of curves is given in Table 3.

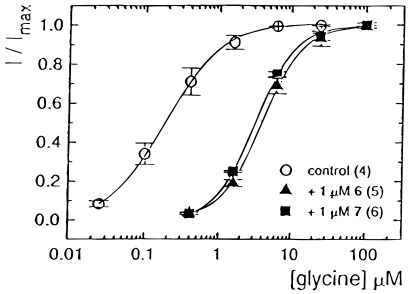

Figure 1. Inhibition of NMDA responses by HBADs **6** and **7** in cultured rat cortical neurons. Steady-state membrane current responses are expressed as a fraction of the maximum response and plotted as the mean ± SEM. Smooth curves are the best individual fits of the logistic equation to the data. Simultaneous fits are not shown. EC_{50} and slope values are, respectively: 0.18 μM and 1.1 for the control curve, 3.9 μM and 1.5 in 1 μM HBAD **6**, 3.2 μM and 1.6 in 1 μM HBAD **7**. K_b values calculated from the simultaneous fits of these data are given in Table 3.

Collectively, the neuronal recordings confirm that **6** and **7** are potent antagonists of NMDA receptors, that the major mechanism of antagonism is competitive inhibition at glycine sites, and that **6** shows a higher degree of steady-state selectivity for NMDA receptors than do previously described HBADs.[9]

In Vivo Measurements

Systemic bioavailability and anticonvulsant effects of three HBADs were measured using a mouse MES model (3 determinations/HBAD).[29,30] For each HBAD, the onset of seizure protection peaked approximately 2 min after iv administration and declined with a biological half-time of approximately 10 min. The ED_{50} values measured at the peak of protection for **6**, **38**, and **52** were 13 (11−17), 6.3 (5.1−7.7), and 3.9 (2.6−5.8) mg/kg, respectively.

Discussion

Structure−Activity Relationship at NMDA Receptor Glycine Sites. The [^{3}H]MK801 assays show that all three 9-substituted HBADs (**36**, **37**, and **39**) are

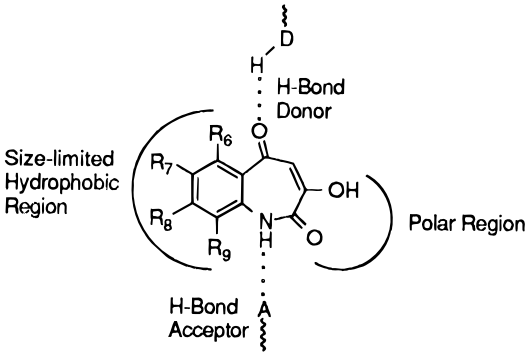

Figure 2. Putative pharmacophore for HBAD NMDA receptor glycine site antagonists (adapted from ref 8b).

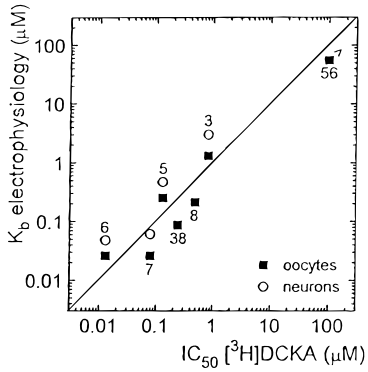

Figure 3. Correlation of HBAD antagonist potency for NMDA receptors as determined by radioligand binding and electrophysiological assays. For radioligand binding studies, IC_{50} values were determined by measuring displacement of [^{3}H]-DCKA from rat brain cortical membranes. For electrophysiological assays, K_b values were estimated from inhibition of NR1a/2C subunit combinations of cloned rat NMDA receptor in *Xenopus* oocytes. In selected cases, K_b values were also estimated from inhibition of NMDA responses in cultured rat cortical neurons; > indicates an indefinite minimum value.

inactive as NMDA receptor antagonists. It seems likely that 9-substitution inhibits hydrogen bonding between the amide proton and a putative hydrogen-bonding site on the glycine receptor[8b] thereby obviating binding (Figure 2). Similar loss or reduction of affinity has been noted for 5,6,7,8-tetrasubstituted QXs[6] and 8-substituted KAs.[28]

In the 7-monosubstituted series, HBADs **14**, **20**, and **21** are inactive as NMDA receptor antagonists in the [^{3}H]MK801 assay. HBADs **13** and **19** have at best weak affinity as determined by [^{3}H]DCKA binding. A similar reduction of potency in the case of **4** versus **3** has been reported.[9] The loss of affinity in this series may be the result of an unfavorable steric interaction of 7-substituents with the binding pocket since, in every HBAD examined, the 7-substituted analog is significantly less potent than the 7-unsubstituted counterpart.

The introduction of a 6-methyl group (**51**) reduces binding affinity by over 1 order of magnitude relative to **3**. This is in contrast to the SAR observed for QXs and KAs where the introduction of Me or Cl at the 5-position (assumed to correspond to the 6-position in the HBAD series) improves the binding affinity.[28] These data suggest that benzazepine type antagonists have a different orientation in the receptor pocket than do other antagonist series. The binding of the 7-membered azepine ring within the hydrophilic portion of the receptor pocket may place C-6 and C-7 in a confined region of the hydrophobic binding pocket (Figure 2).

The most active HBADs incorporate a single substituent at the 8-position. The introduction of a methyl (**5**), chloro (**6**), or bromo (**7**) substituent to this position increases the binding affinity relative to **3**, with **6** and **7** having the highest affinities. These data confirm previous findings[7,9] and are also consistent with the observed SAR for various antagonists at NMDA receptor glycine sites such as 7-substituted QXs,[6] KAs,[28] and 2,3-dihydro-KAs.[31] This suggests that the 8-position in the HBAD series and the 7-position of 6,6-fused ring glycine site antagonists may occupy the same site within the receptor pocket. Interestingly, the 8-F-HBAD **8** has considerably less affinity than **6** or **7**. The modest 2-fold improvement in affinity of **8** compared to **3** likely stems from a positive steric contribution and an unfavorable electronic interaction between the receptor pocket surface and the highly electronegative fluorine atom. A similar trend is observed in the QX series.[6] An ethyl group in the 8-position has a negative effect on the binding affinity with HBAD **60** being 6-fold less potent than **3**. This indicates a size limitation at the 8-position with substituents such as bromo, chloro, and methyl being allowed but larger groups being unfavored. This effect is observed in the KA series.[28]

We have recently shown that multiple substitution in the QX series greatly enhances antagonist potency at NMDA receptor glycine sites.[6] QXs that are trisubstituted in the 5-, 6-, and 7-positions are found to be the most potent. We initially thought that this trend might also apply to the HBAD series. The present study, however, demonstrates that multiple substitution generally results in a reduction of affinity. Dimethyl-substituted HBADs **38** and **52** have approximately one-half the affinity of **5**. In light of the poor affinity of **51**, the affinity of **52** is better than expected. The 6,7-dimethyl HBAD **53** is inactive as a NMDA receptor antagonist. This is not surprising since both 6- and 7-substituents individually have a negative effect on glycine site binding affinity. The poor affinity of trisubstituted HBAD **55** is consistent with these trends.

The binding affinities of analogs with major structural modifications were also determined. The reduced affinity of 4-hydroxy analog **56** relative to **3** suggests that the hydroxyl group of **56** is unable to effectively bind to the proposed polar region of the putative glycine site pharmacophore (Figure 2). Differences in ionizing ability of the two isomers is not likely to be a major factor. The inactivity observed for deshydroxy analog **57** and azepine **58** underscores the binding requirement in the polar and hydrophobic regions, respectively.[32,33] Oxime **59** is also inactive. It is of note that none of the intermediate HBAD methyl ethers act as NMDA receptor antagonists.[34]

Selectivity: NMDA Receptor Glycine Sites versus NMDA Glutamate Sites. There is good agreement between potencies of HBADs estimated by electrophysiological assays and IC_{50} values determined by the [^{3}H]DCKA binding studies (Figure 3). In all cases studied, there is <3-fold difference between the two assay systems. There is no systematic trend within this limited level of discrepancy. The unsubstituted 4-hydroxy analog **56** is essentially inactive in both types of assays. These experiments confirm that HBADs are functional antagonists of NMDA receptors and that

potency of inhibition correlates well with [^{3}H]DCKA binding affinity at glycine sites. A previous study indicates that some HBADs are also low-potency antagonists of NMDA receptor glutamate sites.[9] In the present experiments, the close correlation between glycine site affinity and functional potency implies that inhibition of NMDA responses is predominantly due to effects at glycine sites.

Selectivity: NMDA Glycine Sites versus Non-NMDA Glutamate Receptors. As observed for quinoxaline derivatives,[35] HBAD potencies at AMPA receptors generally correlate with affinities at NMDA receptor glycine sites. In particular, HBADs **6** and **7**, which display the highest affinity as glycine site antagonists, are also the most potent AMPA receptor antagonists. Even with this trend, however, the HBADs with highest affinity for glycine sites still show the highest steady-state selectivity index for NMDA receptors relative to AMPA receptors (Table 3). Levels of selectivity for the less potent HBADs drop to between 20- and 40-fold. As described for quinoxalinediones,[23,29] the functional selectivity of HBADs for glycine and AMPA *in vivo* will depend on additional factors, including the steady-state levels of extracellular glycine and glutamate (relative to their respective EC_{50}s) and the kinetics of receptor equilibration between the agonists and the antagonist. For *in vivo* work, therefore, the moderate potency HBADs are probably best thought of as broad spectrum ionotropic glutamate receptor antagonists.

***In Vivo* Activities of Selected HBADs.** Various examples of potent NMDA receptor glycine site antagonists, such as KAs,[28] 2-carboxytetrahydroquinolines,[31] and many indolecarboxylic acids,[36] demonstrate no significant *in vivo* potency upon systemic administration. It is believed that this lack of bioavailability results from poor compound penetration of the blood−brain barrier. In the present study, mouse MES studies show that HBADs **6**, **38**, and **52** are bioavailable by demonstrating moderately potent anticonvulsant effects after iv administration. Interestingly, the relative *in vivo* potencies of the tested HBADs (**52** > **38** > **6**) are the reverse of the inhibitory potencies measured for these compounds at NMDA and, where tested, AMPA receptors (Tables 2 and 3). This suggests that, within a given compound series, *in vivo* potency is determined by factors other than potency at the receptor.

In the QX series,[6,23,29,37] substituent type and position on the size-limited hydrophobic region are determining factors for bioavailability. Methyl-substituted QXs are generally more bioavailable than the corresponding halogen-substituted analogs. Also, compounds substituted at positions 5 and 7 generally have higher *in vivo* potency than analogs substituted at positions 6 and 7. The present experiments suggest that similar trends are found in the HBAD series, though a larger number of molecules require *in vivo* testing to confirm these relationships.

Summary

HBADs **5**−**7**, which possess an 8-methyl, -chloro, and -bromo substituent, respectively, are the highest affinity benzazepine antagonists for the NMDA receptor glycine sites tested. Replacing these substituents with fluoro or ethyl (**8** or **60**) reduces the binding affinity. Affinity is reduced or eliminated by substitution in the 6-, 7-, or 9-positions, or any combinations thereof, and by repositioning or eliminating the hydroxyl group. Removing the aromatic ring also eliminates affinity. The structural requirements in the size-limited hydrophobic region are more specific in the HBAD series than for other series of NMDA receptor glycine site antagonists such as QXs and KAs. This may be a result of constraints imposed by the 7-membered azepine ring binding in the polar region of these receptors. HBADs are systemically bioavailable with the 6,8-dimethyl-substituted analog **52** possessing the greatest *in vivo* potency.

Experimental Section

Chemistry. Compounds **3**, **5**−**8**, and **56**−**58** were prepared as previously reported.[7,9,10,18−20] Reagents were used as received unless otherwise noted. Melting points were measured on a Thomas Hoover or Mel-Temp melting point apparatus and are uncorrected. For compounds melting above 260 °C, a preheated block was employed. CH_2Cl_2 was distilled from CaH_2 immediately prior to use. Solvent removal was routinely performed on a rotoevaporator at 30−40 °C. All reactions were performed under N_2 unless otherwise noted. TLC analyses were performed on plastic-backed F-254 silica gel plates. ^{1}H and ^{13}C NMR spectra were recorded on a General Electric QE-300 spectrometer. Chemical shifts are reported in δ units referenced to the residual proton or the carbon signal of the deuterated solvent ($CHCl_3$, δ 7.26 or 77.23; CD_3SOCD_2H, δ 2.49 or 39.51). Infrared spectra were obtained on a Nicolet Magna-IR 550 spectrophotometer. MS were recorded on a VG ZAB-2-HF mass spectrometer with a VG-11-250 data system in the electron ionization mode (70 eV). Microanalyses were performed by Desert Analytics, Tuscon, AZ.

3-Methoxy-7-nitro-1*H*-1-benzazepine-2,5-dione (11). To stirred, ice bath cold, concentrated H_2SO_4 (66 mL) was added 2-methoxynaphthalene-1,4-dione[11] (**9**; 10.0 g, 53.1 mmol) in portions to give a deep red solution. NaN_3 (3.80 g, 58.4 mmol) was added in portions. The ice bath was removed, and the reaction mixture was allowed to stir at 25 °C for 20 h. The reaction mixture was recooled in an ice bath, and KNO_3 (5.90 g, 58.4 mmol) was added in small portions. Foaming was noted during this addition. After foaming subsided, the cooling bath was removed and the reaction mixture was allowed to stir at 25 °C for 3.5 h. The reaction mixture was slowly added to crushed ice (200 g) with additional ice being added as needed (final volume 600 mL). The resulting yellow precipitate was collected by filtration to yield a paste. The paste was suspended in water (200 mL) and carefully neutralized with solid $NaHCO_3$. A solution of 30% MeOH/70% $CHCl_3$ (1 L) was added with stirring to dissolve the solid product. The phases were separated, and the organic portion was washed with 30% MeOH/70% H_2O (2 × 500 mL). The organic portion was filtered through cotton, and the solvent was removed. The resulting yellow solid was crystallized from EtOH to yield **11** as near-colorless needles (5.2 g, 40%): mp 252−253 °C; ^{1}H NMR (DMSO-d_6) δ 3.83 (s, 3 H), 6.42 (s, 1 H), 7.55 (d, J = 9.0 Hz, 1 H), 8.40 (dd, J = 9.0, 2.4 Hz, 1 H), 8.70 (d, J = 2.7 Hz, 1 H), 11.84 (s, 1 H); ^{13}C NMR (DMSO-d_6) δ 56.76, 112.4, 122.0, 125.0, 125.7, 127.9, 141.2, 142.5, 156.5, 158.9, 183.0.

7-Bromo-3-methoxy-1*H*-1-benzazepine-2,5-dione (12). To stirred, ice bath cold, concentrated H_2SO_4 (6.6 mL) was added **9** (1.00 g, 5.31 mmol) in portions to give a deep red solution. NaN_3 (690 mg, 10.6 mmol) was added in portions. The ice bath was removed, and the reaction mixture was allowed to stir at 25 °C for 20 h. NBS (1.03 g, 5.80 mmol) was added in one portion, and the reaction mixture was allowed to stir at 25 °C for 48 h. A second portion of NBS (500 mg, 2.81 mmol) was added, and the reaction mixture was allowed to stir for an additional 24 h. The reaction mixture was added to 50 mL of crushed ice, and a solution of 30% MeOH/70% $CHCl_3$ (100 mL) was stirred in. The layers were separated, and the aqueous portion was extracted with 30%

MeOH/70% $CHCl_3$ (3 × 35 mL). The combined organic portion was washed with 30% MeOH/70% H_2O (3 × 50 mL), filtered through a cotton plug, and dried over anhydrous Na_2SO_4. The solvent was removed to yield a yellow solid (900 mg). The solid was heated to boiling in 10% MeOH/90% EtOAc (30 mL) to yield a solid suspended in an orange solution. The solid was collected by filtration, washed with EtOAc, and dried *in vacuo* to yield a yellow powder (120 mg). The powder was crystallized from EtOH to yield **12** as gold plates (94 mg, 6%): mp 290−291 °C dec; ^{1}H NMR (DMSO-d_6) δ 3.80 (s, 3 H), 6.36 (s, 1 H), 7.35 (d, J = 8.7 Hz, 1 H), 7.78 (dd, J = 8.7, 2.1 Hz, 1 H), 7.99 (d, J = 2.1 Hz, 1 H), 11.45 (s, 1 H). Anal. ($C_{11}H_8BrNO_3$) C, H, N.

7-Amino-3-methoxy-1*H*-1-benzazepine-2,5-dione (15). A mixture of **11** (250 mg, 1.01 mmol), quinoline (20 mg), and Pd/C (10%, 100 mg) in CH_2Cl_2/MeOH (1:1, 250 mL) was hydrogenated (Parr) at 5 psig for 1 h at 25 °C. The catalyst was removed by filtration (Celite), and the solvent was removed to yield **15** as an orange powder. This was combined with an identically prepared portion of **15** and was crystallized from MeOH/EtOAc (1:1) to yield **15** as an orange solid (170 mg, 39%): mp 247−249 °C dec; ^{1}H NMR (DMSO-d_6) δ 3.76 (s, 3 H), 5.31 (s, 2 H), 6.28 (s, 1 H), 6.85 (dd, J = 8.7, 2.7 Hz, 1 H), 7.03−7.15 (m, 2 H), 11.01 (s, 1 H). Anal. ($C_{11}H_{10}N_2O_3$) C, H, N.

7-Acetamido-3-methoxy-1*H*-1-benzazepine-2,5-dione (16). Hydrogenation of **11** (400 mg, 1.61 mmol) was performed as described for **15**. After filtration of the catalyst, acetic anhydride (3 mL) was added to the filtrate and the resulting solution was allowed to stir for 1 h at 25 °C to yield a yellow, cloudy mixture. The mixture was filtered, and the solvent was removed from the filtrate to yield **16** as a yellow powder (386 mg, 92%; ∼90% pure by ^{1}H NMR and suitable for use in the next reaction without further purification). An analytical sample was prepared by crystallization from EtOH: mp 304−306 °C dec; ^{1}H NMR (DMSO-d_6) δ 2.03 (s, 3 H), 3.79 (s, 3 H), 6.34 (s, 1 H), 7.33 (d, J = 8.7 Hz, 1 H), 7.80 (dd, J = 8.7, 2.1 Hz, 1 H), 8.13 (d, J = 1.8 Hz, 1 H), 10.13 (s, 1 H), 11.28 (s, 1 H). Anal. ($C_{13}H_{12}N_2O_4$) C, H, N.

7-(Trifluoroacetamido)-3-methoxy-1*H*-1-benzazepine-2,5-dione (17). Hydrogenation of **11** (400 mg, 1.61 mmol) was performed as described for **15**. After filtration of the catalyst, the solvent was removed from the filtrate to yield an orange solid. This solid was dissolved in boiling EtOAc (700 mL), filtered while hot, and allowed to cool to 25 °C to give a clear, orange solution. TFAA (0.5 mL) was added, and the reaction mixture was allowed to stir at 25 °C for 1 h, at which point a yellow precipitate was present. The solvent was removed to yield a yellow solid. Crystallization from EtOH yielded **17** as yellow plates (260 mg, 52%): ^{1}H NMR (DMSO-d_6) δ 3.80 (s, 3 H), 6.37 (s, 1 H), 7.42 (d, J = 8.7 Hz, 1 H), 7.87 (dd, J = 8.7, 2.4 Hz, 1 H), 8.28 (d, J = 2.1 Hz, 1 H), 11.41 (s, 1 H), 11.44 (s, 1 H). A portion was recrystallized from EtOH: mp 327−328 °C dec. Anal. ($C_{13}H_9F_3N_2O_4$) C, H, N.

7-Azido-3-hydroxy-1*H*-1-benzazepine-2,5-dione (21). Hydrogenation of **11** (400 mg, 1.61 mmol) was performed as described for **15**. After filtration of the catalyst, the solvent was removed from the filtrate to yield an orange solid. This solid was dissolved in boiling EtOAc (700 mL), filtered while hot, and allowed to cool to 25 °C to give a clear, orange solution. The solution was made acidic by the addition of anhydrous HCl at 25 °C. Solvent removal yielded an orange/brown powder (382 mg) which was utilized without further purification. A portion (125 mg, 491 μmol) was suspended in water (19 mL) and cooled in an ice bath. Concentrated HCl (9 mL) was added while maintaining the temperature between 0 and 5 °C. A solution of $NaNO_2$ (37 mg, 540 μmol) in water (1 mL) was added in one portion. The reaction mixture was allowed to stir between 0 and 5 °C for 1 h to yield a near-homogeneous yellow solution. Solid NaN_3 (35 mg, 540 μmol) was added in one portion. The ice bath was removed, and the reaction mixture was allowed to warm with stirring to 20 °C over a 2 h period. The resulting precipitate was collected, washed with water (6 × 2 mL), and dried *in vacuo* to yield a brown powder (50 mg). A second portion of amine hydrochloride (231 mg, 909 μmol) was treated in a similar manner to yield an additional 80 mg of crude product. The combined brown powder consisted of **18**, **21**, and side products as determined by TLC (57% 2-propanol, 20% dioxane, 11.5% water, 11.5% NH_4OH). The side products were removed by dissolving the powder in boiling EtOH (75 mL), concentrating the resulting solution to 25 mL, and allowing the concentrate to cool to 25 °C. A precipitate formed which was collected by filtration to yield 91 mg of a brown powder. The powder was dissolved in boiling EtOH (100 mL). The resulting solution was allowed to stir for 1 min at 25 °C; then a solution of 10% H_2SO_4/90% water (10 mL) was added. The reaction mixture was allowed to stir for 5 min at 25 °C; then an additional portion of the acid solution (90 mL) was added. A precipitate formed after a few minutes. After 12 min of total reaction time, the mixture was added to crushed ice (50 mL) and the EtOH was removed. The solid was collected and washed with water (10 × 2 mL). The damp filter cake was crystallized from EtOH to yield **21** as an orange crystalline solid (55 mg, 18%): mp 190 °C dec (without melting); ^{1}H NMR (DMSO-d_6) δ 6.42 (s, 1 H), 7.39 (dd, J = 8.7, 2.7 Hz, 1 H), 7.51 (d, J = 8.7 Hz, 1 H), 7.66 (d, J = 2.7 Hz, 1 H), 10.78 (bs, 1 H), 11.70 (s, 1 H); IR (KBr) 2116 cm^{-1} (N_3). Anal. ($C_{10}H_6N_4O_3$) C, H, N.

General Method for the Preparation of 2-Methoxynaphthalene-1,4-diones via a Diels−Alder Reaction of 2-Methoxybenzoquinone (26): Synthesis of 2-Methoxy-6,8-dimethylnaphthalene-1,4-dione (29). A suspension of **26**[13] (4.90 g, 35.5 mmol), 1,3-dimethylbuta-1,3-diene (**23**; 25 mL, technical grade), and hydroquinone (500 mg) in toluene (50 mL) was stirred at 60 °C for 20 h. The resulting pale orange, near-homogeneous solution was allowed to cool to 25 °C. The reaction mixture was filtered, and the solvent was removed to give an orange solid (9.3 g). Without purification, the solid was dissolved in MeOH (a gummy colorless solid that failed to dissolve was removed by filtration). Et_3N (3 mL) was added, and the resulting dark solution was allowed to stir vigorously under O_2 for 2.5 h at 25 °C. The reaction mixture was acidified with 10% HCl (100 mL) and diluted with water (200 mL). The MeOH was removed to give an orange suspension. The suspension was extracted with $CHCl_3$ (3 × 100 mL). The extract was washed with saturated $NaHCO_3$ (3 × 75 mL) and water (1 × 200 mL) and filtered through cotton. The solvent was removed to give an orange solid (5.9 g). Crystallization from EtOH yielded **29** as yellow needles (2.79 g, 36%): mp 176−177 °C; ^{1}H NMR ($CDCl_3$) δ 2.44 (s, 3 H), 2.72 (s, 3 H), 3.88 (s, 3 H), 6.10 (s, 1 H), 7.30 (s, 1 H), 7.82 (s, 1 H).

5,8-Dihydro-2-methoxy-5,8-dimethylnaphthalene-1,4-dione (27). Dione **27** was prepared in a manner similar to that described for **29** with the crude product being purified chromatographically (silica gel/$CHCl_3$) prior to crystallization to yield **27** as orange plates (2.22 g, 46%): mp 110−112 °C; ^{1}H NMR ($CDCl_3$) δ 1.19 (s, 3 H), 1.21 (s, 3 H), 3.39−3.42 (m, 2 H), 3.81 (s, 3 H), 5.75−5.85 (m, 2 H), 5.88 (s, 1 H).

2-Methoxy-5,8-dimethylnaphthalene-1,4-dione (31). A suspension of **27** (500 mg, 2.29 mmol) and DDQ (1.30 g, 5.72 mmol, freshly crystallized from toluene) in toluene (12 mL) was heated at reflux for 2.6 h. The reaction mixture was allowed to cool to 25 °C. The suspended material was removed by filtration and washed with fresh toluene (4 × 3 mL). The toluene was removed, and the residue was dissolved in $CHCl_3$ (60 mL). This solution was washed with 25% saturated $NaHCO_3$ (5 × 40 mL) and 50% saturated brine (1 × 40 mL) and filtered through cotton. The solvent was removed to give a dark brown solid (442 mg, 89% crude yield). A total of 980 mg of crude material was passed through a silica gel column (2.5 × 25 cm) with $CHCl_3$ elution to give a green solid (906 mg). Crystallization from EtOH yielded **31** as a greenish-yellow crystalline solid (612 mg, 62% from crude material): mp 145−146 °C; ^{1}H NMR ($CDCl_3$) δ 2.71 (s, 6 H), 3.86 (s, 3 H), 6.06 (s, 1 H), 7.35 (d, J = 8.1 Hz, 1 H), 7.39 (d, J = 8.1 Hz, 1 H).

2-Bromo-5-methoxyhydroquinone (41). To a stirred, water bath-cooled (15−20 °C) solution of 2-methoxyhydroquinone[17] (**40**; 20.0 g, 143 mmol) in glacial AcOH (400 mL) was added Br_2 (7.50 mL, 23.3 g, 146 mmol) dropwise over 20 min. The color of the reaction mixture darkened during the

addition. TLC (5% EtOAc/95% $CHCl_3$) indicated the formation of one major higher R_f spot and one minor higher R_f spot relative to **40**. The solvent was removed to give a dark brown solid. The solid was dissolved in hot $CHCl_3$ (400 mL) and filtered through a pad of silica gel (8 × 8 cm). The solvent was removed to give a tan solid. Crystallization from benzene yielded **41** as brown to purple needles (24.5 g, 78%): mp 127−128 °C; ^{1}H NMR ($CDCl_3$) δ 3.86 (s, 3 H), 5.12 (bs, 1 H), 5.23 (bs, 1 H), 6.60 (s, 1 H), 7.00 (s, 1 H).

2-Bromo-5-methoxybenzoquinone (42). A solution of **41** (4.00 g, 18.3 mmol) in $CHCl_3$ (150 mL, prepared with warming) was allowed to vigorously stir with a solution of $NaIO_4$ (7.81 g, 36.5 mmol) in water (200 mL) at 25 °C. The reaction mixture immediately turned dark and then became orange over a period of time. After 30 min, the layers were separated and the aqueous portion was extracted with $CHCl_3$ (1 × 30 mL). The combined $CHCl_3$ portion was washed with brine (1 × 30 mL) and filtered through cotton. The solvent was removed to yield **42** as a yellow solid which was of sufficient purity for further reaction (4.00 g, 100%): mp 184−186 °C. Crystallization of a portion from MeOH yielded **42** as orange needles: mp 186−187 °C (lit.[16] mp 190−191 °C); ^{1}H NMR ($CDCl_3$) δ 3.86 (s, 3 H), 6.12 (s, 1 H), 7.24 (s, 1 H).

General Method for the Preparation of 2-Methoxynaphthalene-1,4-diones via a Diels−Alder Reaction of 42: Synthesis of 2-Methoxy-5-methylnaphthalene-1,4-dione (43). A suspension of **42** (4.0 g, 18 mmol) and *trans*-piperylene (**22**; 5.5 mL, 3.7 g, 47 mmol, technical grade) in toluene (100 mL) was allowed to stir at 60−70 °C for 4 days. A homogeneous solution was present. The status of the reaction was determined by ^{1}H NMR. Since the adduct was not stable once the reaction solvent was evaporated, an aliquot was diluted in half with MeOH and treated with an excess of Et_3N. After 1 min, dilute HCl was added and the mixture extracted with $CHCl_3$. The extract was washed with water and filtered through cotton. The solvent was removed. The ^{1}H NMR was determined in $CDCl_3$. The absence of a resonance at 7.24 ppm indicated that the starting quinone was totally consumed. The remaining reaction mixture was allowed to cool to 25 °C and diluted with MeOH (100 mL). The reaction mixture was purged with N_2 for 5 min with stirring, and Et_3N (3.69 g, 36.5 mmol) was added. The reaction mixture darkened. The reaction mixture was allowed to stir for 5 min. Dilute HCl (150 mL) was added with stirring to give a lighter yellow/orange mixture. The layers were separated, and the aqueous portion was extracted with toluene (1 × 30 mL). The combined toluene portion was washed with water and brine (30 mL each) and filtered through cotton. The solvent was removed to give an orange solid (4.2 g). Crystallization from EtOH yielded the 5,8-dihydro analog of **43** as an orange crystalline solid (2.87 g, 77%): mp 116−117 °C (lit.[15] mp not reported); ^{1}H NMR ($CDCl_3$) δ 1.17 (d, J = 6.9 Hz, 3 H), 2.86−3.01 (m, 1 H), 3.09−3.24 (m, 1 H), 3.36−3.50 (m, 1 H), 3.80 (s, 3 H), 5.75−5.82 (m, 2 H), 5.88 (s, 1 H).

A solution of the above material (100 mg, 490 μmol) in $CHCl_3$ (5 mL) was refluxed in the presence of MnO_2 (213 mg, 2.45 mmol) for 45 min (the progress of the reaction was monitored by ^{1}H NMR). The reaction mixture was allowed to cool to 25 °C and filtered through a pad of Celite. Solvent removal yielded **43** as a yellow powder (99 mg, 100%): mp 139−140 °C; ^{1}H NMR ($CDCl_3$) δ 2.76 (s, 3 H), 3.88 (s, 3 H), 6.11 (s, 1 H), 7.50−7.59 (m, 2 H), 8.07 (dd, J = 6.6, 1.8 Hz, 1 H). A portion crystallized from MeOH yielded **43** as orange needles: mp 140−141 °C.

General Method for the Schmidt Reaction of 2-Methoxynaphthalene-1,4-diones: Synthesis of 3-Methoxy-9-methyl-1*H*-1-benzazepine-2,5-dione (32). To stirred, ice bath cold CF_3SO_3H (3.0 mL) was added 2-methoxy-8-methylnaphthalene-2,5-dione (**28**; 483 mg, 2.39 mmol) in portions. A deep red solution resulted. To this cold solution was added NaN_3 (186 mg, 2.87 mmol) in portions. The reaction mixture was allowed to slowly warm to 25 °C with stirring under N_2. Gas evolution was noted. After 24 h, the reaction was judged complete by TLC (10% EtOAc/90% $CHCl_3$). The reaction mixture was added to stirred ice water (30 mL) to give a green suspension. This was extracted with 30% MeOH/70% $CHCl_3$ (4 × 25 mL) to give a green organic solution. This was washed with water (3 × 50 mL) and filtered through cotton. The solvent was removed to give a purple solid (500 mg). The product was purified by chromatography on silica gel (2.5 × 25 cm) with $CHCl_3$ elution give an orange solid (367 mg). Crystallization from EtOH yielded **32** as beige needles (245 mg, 47%). A portion was recrystallized from EtOH to yield **32** as near-colorless needles: mp 188−189 °C; ^{1}H NMR (DMSO-d_6) δ 2.41 (s, 3 H), 3.75 (s, 3 H), 6.26 (s, 1 H), 7.18 (t, J = 7.8 Hz, 1 H), 7.46 (d, J = 7.5 Hz, 1 H), 7.52 (d, J = 8.1 Hz, 1 H), 9.45 (s, 1 H); MS m/z 217 (M^+, 100).

3-Methoxy-6,8-dimethyl-7-nitro-1*H*-1-benzazepine-2,5-dione (54). Methyl ether **54** was prepared from **49** (prepared *in situ* from **44**, 1.00 g, 4.63 mmol) employing methods described for the preparation of **11** to yield **54** as an orange solid (668 mg, 52%): mp 262−266 °C dec; ^{1}H NMR (DMSO-d_6) δ 2.17 (3 H), 2.23 (3 H), 3.73 (3 H), 6.38 (s, 1 H), 7.18 (s, 1 H), 11.25 (s, 1 H); ^{13}C NMR (DMSO-d_6) δ 14.88, 16.85, 56.35, 113.2, 120.7, 128.6, 128.8, 132.2, 136.0, 148.9, 154.4, 160.1, 189.6. A portion recrystallized from EtOH yielded **54** as a beige powder: mp 268−271 °C dec.

General Method A for the Demethylation of 3-Methoxy-1*H*-1-benzazepine-2,5-diones: Synthesis of 3-Hydroxy-7-nitro-1*H*-1-benzazepine-2,5-dione (13). A solution of **11** (225 mg, 907 μmol) in 80 mL of boiling EtOH was prepared. The solution was stirred without heating for 1 min; then a solution of 10% aqueous H_2SO_4 (10 mL) was added. The reaction mixture was allowed to stir for 5 min; then additional acid solution (70 mL) was added. Further stirring for 10 min yielded a near-colorless precipitate. The reaction mixture was added to crushed ice, and the ethanol was removed. The precipitate was collected and washed with water (5 × 5 mL). The damp filter cake was crystallized from EtOH to yield **13** as colorless needles (124 mg, 58%): mp 250 °C dec (without melting); ^{1}H NMR (DMSO-d_6) δ 6.45 (s, 1 H), 7.61 (d, J = 9.0 Hz, 1 H), 8.39 (dd, J = 9.0, 2.7 Hz, 1 H), 8.79 (d, J = 2.7 Hz, 1 H), 11.14 (bs, 1 H), 12.04 (s, 1 H). Anal. ($C_{10}H_6N_2O_5$) C, H, N.

General Method B for the Demethylation of 3-Methoxy-1*H*-1-benzazepine-2,5-diones: Synthesis of 3-Hydroxy-9-methyl-1*H*-1-benzazepine-2,5-dione (36). To a stirred suspension of **32** (200 mg, 921 μmol) in CH_2Cl_2 (2 mL) was added a solution of BBr_3 in CH_2Cl_2 (2 mL, 1 M) in one portion at 25 °C. The reaction mixture instantaneously became homogeneous and yellow; then a yellow precipitate formed after a few seconds. The reaction mixture was allowed to stir at 25 °C for 45 min. The reaction mixture was added to saturated $NaHCO_3$ (15 mL), and the resulting beige suspension was allowed to stir for 15 min to give a cloudy, orange solution. The solution was filtered. The filtrate was acidified with concentrated HCl to a pH of 2. The resulting precipitate was collected by filtration and washed with water (5 × 2 mL). The damp filter cake was crystallized from EtOH to yield **36** as brown needles (98 mg, 52%): mp 184−186 °C dec; ^{1}H NMR (DMSO-d_6) δ 2.46 (s, 3 H), 6.28 (s, 1 H), 7.19 (t, J = 7.5 Hz, 1 H), 7.48 (d, J = 7.2 Hz, 1 H), 7.67 (d, J = 7.8 Hz, 1 H), 9.94 (s, 1 H), 10.85 (bs, 1 H). Anal. ($C_{11}H_9NO_3 \cdot 0.50\ H_2O$) C, H, N.

1*H*-1-Benzazepine-2,3,4,5-tetrone 4-Oxime (59). A mixture of **3** (188 mg, 1.00 mmol) and $NaNO_2$ (182 mg, 2.64 mmol) in 0.1 M aqueous NaOH (6 mL) was allowed to stir at room temperature for 1 h. The resulting mixture was treated with 2 M aqueous H_2SO_4 (2 mL) and allowed to stir for 3 h at room temperature. The reaction mixture was treated with a solution of $NaNO_2$ (181 mg, 2.62 mmol) in water (2 mL) and allowed to stir overnight at room temperature. The reaction mixture was treated every 24 h with a solution of $NaNO_2$ (100 mg, 1.45 mmol) in water (0.5 mL) for 7 days. After the final addition, the reaction mixture was allowed to stir for an additional 24 h to yield a suspension. The solid was collected by filtration, washed with water, and dried *in vacuo* to yield **59** as a pale yellow solid (149 mg, 68%): mp 196−197 °C; ^{1}H NMR (DMSO-d_6) δ 7.16−7.23 (m, 2 H), 7.55 (t, J = 7.5 Hz, 1 H), 7.96 (d, J = 7.8 Hz, 1 H), 10.49 (s, 1 H), 12.00 (s, 1 H). Anal. ($C_{10}H_6N_2O_4 \cdot 1.10H_2O$) C, H, N.

[^{3}H]MK801 Assay. This assay was performed with rat brain cortical membranes employing methods previously described.[21]

[^{3}H]DCKA Assay. This assay was performed as previously described.[22] Briefly, [^{3}H]DCKA (15−20 nM) was incubated with well-washed rat brain cortical membranes and nine concentrations (up to 100 μM) of HBAD in 50 mM HEPES-KOH, pH 7.5, buffer. Following a 30 min incubation on ice, the assays were terminated by filtration and the filter-bound radioactivity was determined by liquid scintillation counting. The IC_{50} (concentration of test compound producing 50% inhibition of specific binding) was estimated using the sigmoidal equation (Prism Graph Pad).

Electrophysiology and Data Analysis. Methods for RNA preparation, dissection and microinjection of *Xenopus* oocytes, two-electrode voltage-clamp recordings, and preparation of HBAD stock solutions were as described in Woodward et al.[23] Methods for culturing rat cortical neurons and for whole cell clamp recordings were as described in Huettner and Baughman.[38]

In oocyte experiments, concentration−response data for glycine and AMPA and concentration−inhibition curves for HBADs were all fit with logistic equations.[23] The EC_{50} and slope values for glycine at NR1a/2C receptors were 0.174 μM and 1.45 ($n = 6$). The EC_{50} and slope values for AMPA were 5.89 μM and 1.96 ($n = 5$). These values were used in all subsequent calculations of HBAD antagonist potency. K_b values were calculated from concentration−inhibition curves using a generalized form of the Cheng−Prusoff equation:[26]

$$K_b = \frac{IC_{50}}{\{2 + ([\text{agonist}]_f/EC_{50})^n\}^{1/n} - 1}$$

where IC_{50} is the concentration of HBAD that reduces control response by 50%, $[\text{agonist}]_f$ is the concentration of agonist used for the control response, EC_{50} is the concentration of agonist (glycine or AMPA) that elicits a half-maximal response, and n is the slope factor of the agonist concentration−response relation. Fixed agonist concentrations were 1 μM glycine plus 100 μM glutamate for NR1a/2C receptors. The control membrane current range in these experiments was 71−589 nA, and the mean response was 140 ± 20 nA ($n = 27$). The fixed agonist concentration was 10 μM AMPA for AMPA receptors. The current range in these experiments was 99−200 nA, and the mean response was 150 ± 4 ($n = 28$). The holding potential for all measurements was −70 mV.

K_b values in the neuronal recordings were determined from simultaneous fit of concentration−response data under control conditions and in the presence of a fixed concentration of HBAD.[9] Current ranges for these experiments were 323−1530 pA for glycine/NMDA (100 μM), and 205−1800 pA for kainate. Mean responses were 729 ± 150 pA ($n = 15$) and 534 ± 108 pA ($n = 18$), respectively. The holding potential for all experiments was −70 mV. Statistical conformity to the competitive model was determined by F-test.[9] F values are given in the form $F_{(df_2-df_1),df_1}$, where d_{f1} is the degree of freedom in the individual fits, and d_{f2} is the degree of freedom in the simultaneous fit. Other data are given as mean ± SEM.

Mouse MES Studies. General methods for MES studies were performed as previously reported.[29,30] Briefly, seizures were induced in male Swiss Webster mice (body weight 23−27 g, housed with *ad libitum* food and water) via corneal electrodes (ECT 7801, Ugo Basile). Rectangular pulses (50 mA, 60−75 Hz, 0.8 ms width, 0.2 s train length) were employed. Seizure occurrence was recorded as a tonic hindlimb extension after electroshock stimulus. HBADs were formulated for iv administration as 5 mg/mL solutions in 0.2 M tris(hydroxymethyl)aminomethane. The vehicle alone induced no detectable levels of protection. ED_{50} values and 95% confidence intervals were calculated by Litchfield and Wilcoxon analysis (MicroComputer Specialists, Philadelphia, PA).

Acknowledgment. Financial support was provided by CoCensys, Inc. and by National Institutes of Health Grants NS 30888 (J.E.H.) and DA 06726 (E.W., J.F.W.K.). We thank Dr. John Guastella (CoCensys) for the preparation of NMDA receptor (NR1a/2C) cRNA, Sylvia Loyola (University of California, Irvine) for the [^{3}H]MK801 binding determinations, Prof. Ricardo Miledi and Dr. Yan Ni (University of California, Irvine) for the gift of rat brain poly(A)$^+$ RNA, Prof. Alun H. Rees (Trent University, Peterborough, Ontario, Canada) for providing compound **60**, Dr. Peter H. Seeburg (University of Heidelberg, Heidelberg, Germany) for the NMDA receptor clones, and Dr. Timothy Weakley (University of Oregon) for the X-ray crystallographic determinations.

Supporting Information Available: Accounts of structural analyses and listings of crystallographic properties and numerical details of refinement, atomic coordinates, bond lengths and angles, anisotropic thermal parameters, contact distances, torsion angles, and mean planes, together with ORTEP diagrams for compounds **11** and **36** and tables of physical data, NMR spectroscopic data and methods of preparation for substituted 2-methoxynaphthalene-1,4-diones and HBAD 3-methyl ethers (30 pages); observed and calculated structure factors (27 pages). Ordering information is given on any current masthead page.

References

(1) Watkins, J. C. The NMDA Receptor Concept: Origins and Development. In *The NMDA Receptor*, 2nd ed.; Collingridge, G. L., Watkins, J. C., Eds.; Oxford University Press: Oxford, 1994; pp 1−30.

(2) (a) McCulloch, J. Excitatory Amino Acid Antagonists and Their Potential for the Treatment of Ischemic Brain Damage in Man. *Br. J. Clin. Pharmacol.* **1992**, *34*, 106−114. (b) Dodd, P. R.; Scott, H. L.; Westphalen, R. I. Excitotoxic Mechanisms in the Pathogenesis of Dementia. *Neurochem. Int.* **1994**, *25*, 203−219. (c) Lipton, S. A. Models of Neuronal Injury in AIDS: Another Role for the NMDA Receptor? *Trends Neurosci.* **1992**, *15*, 75−79.

(3) (a) Choi, D. W.; Rothman, S. M. The Role of Glutamate Neurotoxicity in Hypoxic-Ischemic Neuronal Death. *Annu. Rev. Neurosci.* **1990**, *13*, 171−182. (b) Meldrum, B.; Garthwaite, J. Excitatory Amino Acid Neurotoxicity and Neurodegenerative Disease. *Trends Pharmacol. Sci.* **1990**, *11*, 379−387.

(4) (a) Johnson, J. W.; Ascher, P. Glycine Potentiates the NMDA Response in Cultured Mouse Brain Neurons. *Nature (London)* **1987**, *325*, 529−531. (b) Kleckner, N. W.; Dingledine, R. Requirement for Glycine in Activation of NMDA-Receptors Expressed in *Xenopus* Oocytes. *Science (Washington, D.C.)* **1988**, *241*, 835−837.

(5) Kulagowski, J. J.; Baker, R.; Curtis, N. R.; Leeson, P. D.; Mawer, I. M.; Moseley, A. M.; Ridgill, M. P.; Rowley, M.; Stansfield, I.; Foster, A. C.; Grimwood, S.; Hill, R. G.; Kemp, J. A.; Marshall, G. R.; Saywell, K. L.; Tricklebank, M. D. 3′-(Arylmethyl)- and 3′-(Aryloxy)-3-phenyl-4-hydroxyquinoline-2(1*H*)-ones: Orally Active Antagonists of the Glycine Site on the NMDA Receptor. *J. Med. Chem.* **1994**, *37*, 1402−1405.

(6) Keana, J. F. W.; Kher, S. M.; Cai, S. X.; Dinsmore, C. M.; Glenn, A. G.; Guastella, J.; Huang, J.-C.; Ilyin, V.; Lü, Y.; Mouser, P. L.; Woodward, R. M.; Weber, E. Synthesis and Structure-Activity Relationships of Substituted 1,4-Dihydroquinoxaline-2,3-diones: Antagonists of *N*-Methyl-D-Aspartate (NMDA) Receptor Glycine Sites and of Non-NMDA Glutamate Receptors. *J. Med. Chem.* **1995**, *38*, 4367−4379.

(7) Chapdelaine, M. J.; McLaren, C. D. Therapeutic Benzazarine Compounds. U.S. Patent 5,254,683, Oct. 19, 1993.

(8) (a) Leeson, P. D. Glycine-Site *N*-Methyl-D-Aspartate Receptor Antagonists. In *Drug Design for Neuroscience;* Kozikowski, A. P., Ed.; Raven Press: New York, 1993; pp 339−381. (b) Leeson P. D.; Iversen, L. L. The Glycine Site on the NMDA Receptor: Structure-Activity Relationships and Therapeutic Potential. *J. Med. Chem.* **1994**, *37*, 4053−4067. (c) Iversen, L. L.; Kemp, J. A. Non-Competitive NMDA Antagonists as Drugs. In *The NMDA Receptor*, 2nd ed.; Collingridge, G. L., Watkins, J. C., Eds.; Oxford University Press: Oxford, 1994; pp 469−486.

(9) Swartz, K. J.; Koroshetz, W. J.; Rees, A. H.; Huettner, J. E. Competitive Antagonism of Glutamate Receptor Channels by Substituted Benzazepines in Cultured Cortical Neurons. *Mol. Pharmacol.* **1992**, *41*, 1130−1141.

(10) Birchall, G. R.; Rees, A. H. Some Derivatives of 1-Benzazepine. Part II. *Can. J. Chem.* **1974**, *52*, 610−615.
(11) Fieser, L. F. Alkylation of Hydroxynaphthoquinones I. Ortho-Esters. *J. Am. Chem. Soc.* **1926**, *48*, 2922−2937.
(12) Bohlmann, F.; Mathar, W.; Schwarz, H. Über die Regioselektivität von Diensynthesen Substituierter Chinone. (Regioselectivity of diene syntheses of substituted quinones.) *Chem. Ber.* **1977**, *110*, 2028−2045.
(13) Adler, E.; Magnusson, R. Periodate Oxidation of Phenols I. Monoethers of Pyrocatechol and Hydroquinone. *Acta Chem. Scand.* **1959**, *13*, 505−519.
(14) Trave, R.; Garanti, L.; Pavan, M. The Chemical Constitution of the Venom of the Myriapod Archiulus Sabulosus. *Chim. Ind. (Milan)* **1959**, *41*, 19−29.
(15) Tegmo-Larsson, I.-M.; Rozeboom, M. D.; Houk, K. N. Regioselectivities of Diels-Alder Cycloadditions to Methoxy-Substituted Quinones. *Tetrahedron Lett.* **1981**, *22*, 2043−2046.
(16) Blatchly, J. M.; Green, R. J. S.; McOmie, J. F. W.; Searle, J. B. Thiele Acetylation of Quinones. Part III. *p*-Benzoquinones with Bromo- and Methoxy-Substituents. *J. Chem. Soc. C* **1969**, 1353−1358.
(17) Logan, C. D.; Husband, R. M.; Purves, C. B. Studies in the Polyoxyphenol Series VIII. The Oxidation of Substances Related to Vanillin with Sodium Chlorite and Chlorine Dioxide. *Can. J. Chem.* **1955**, *33*, 82−96.
(18) Moore, H. W.; Shelden, H. R.; Weyler, W., Jr. Rearrangement of Azidoquinones IV. Ring Expansion of 4-Azido-1,2-naphthoquinone. *Tetrahedron Lett.* **1969**, *16*, 1243−1246.
(19) Moriconi, E. J.; Maniscalco, I. A. π-Equivalent Heterocyclic Congeners of Tropone. Azatropones. *J. Org. Chem.* **1972**, *37*, 208−215.
(20) Hughes, C. G.; Lewars, E. G.; Rees, A. H. Azatropolones. Part II. The Schmidt Reaction of 2-Methoxy-5-methylbenzoquinone. *Can. J. Chem.* **1974**, *52*, 3327−3330.
(21) Kaneko, S.; Sugimura, M.; Inoue, T.; Satoh, M. Effects of Several Cerebroprotective Drugs on NMDA Channel Function: Evaluation Using *Xenopus* Oocytes and [^{3}H]MK-801 Binding. *Eur. J. Pharmacol., Mol. Pharmacol. Sect.* **1991**, *207*, 119−128.
(22) Canton, T.; Doble, A.; Miquet, J. M.; Jimonet, P.; Blanchard, J. C. A Rapid Filtration Assay for the Glycine Binding Site on the NMDA Receptor in Rat Cortical Membranes using [^{3}H]Dichlorokynurenic Acid. *J. Pharm. Pharmacol.* **1992**, *44*, 812−816.
(23) Woodward, R. M.; Huettner, J. E.; Guastella, J.; Keana, J. F. W.; Weber, E. *In Vitro* Pharmacology of ACEA-1021 and ACEA-1031: Systemically Active Quinoxalinediones with High Affinity and Selectivity for *N*-Methyl-D-Aspartate Receptor Glycine Sites. *Mol. Pharmacol.* **1995**, *47*, 568−581.
(24) Monyer, H.; Sprengel, R.; Schoepfer, R.; Herb, A.; Higuchi, M.; Lomeli, H.; Burnashev, N.; Sakmann, B.; Seeburg, P. H. Heteromeric NMDA Receptors: Molecular and Functional Distinction of Subtypes. *Science (Washington, D.C.)* **1992**, *256*, 1217−1221.
(25) Sugihara, H.; Moriyoshi, K.; Ishii, T.; Masu, M.; Nakanishi, S. Structures and Properties of Seven Isoforms of the NMDA Receptor Generated by Alternative Splicing. *Biochem. Biophys. Res. Commun.* **1992**, *185*, 826−832.
(26) Leff, P.; Dougall, I. G. Further Concerns Over Cheng-Prusoff Analysis. *Trends Pharmacol. Sci.* **1993**, *14*, 110−112.
(27) Cai, S. X.; Zhou, Z.-L.; Huang, J.-C.; Whittenmore, E. R.; Egbuwoku, Z. O.; Lü, Y.; Hawkinson, J. E.; Woodward, R. M.; Weber, E.; Keana, J. F. W. Synthesis and Structure-Activity Relationships of 1,2,3,4-Tetrahydroquinoline-2,3,4-trione-3-oximes: Novel and Highly Potent Antagonists for NMDA Receptor Glycine Sites. *J. Med. Chem.* **1996**, *39*, 3248−3255.
(28) Leeson, P. D.; Baker, R.; Carling, R. W.; Curtis, N. R.; Moore, K. W.; Williams, B. J.; Foster, A. C.; Donald, A. E.; Kemp, J. A.; Marshall, G. R. Kynurenic Acid Derivatives. Structure-Activity Relationships for Excitatory Amino Acid Antagonism and Identification of Potent and Selective Antagonists at the Glycine Site on the *N*-Methyl-D-Aspartate Receptor. *J. Med. Chem.* **1991**, *34*, 1243−1252.
(29) Woodward, R. M.; Huettner, J. E.; Tran, M.; Guastella, J.; Keana, J. F. W.; Weber, E. Pharmacology of 5-Chloro-7-trifluoromethyl-1,4-dihydro-2,3-quinoxalinedione: A Novel Systemically Active Ionotropic Glutamate Receptor Antagonist. *J. Pharmacol. Exp. Ther.* **1995**, *275*, 1209−1218.
(30) Swinyard, E. A. Assay of Antiepileptic Drug Activity in Experimental Animals: Standard Tests. In *Anticonvulsant Drugs. International Encyclopedia of Pharmacology and Therapeutics*; Mercier, J., Ed.; Pergamon Press: Oxford, 1972; pp 47−65.
(31) Carling, R. W.; Leeson, P. D.; Moseley, A. M.; Baker, R.; Foster, A. C.; Grimwood, S.; Kemp, J. A.; Marshall, G. R. 2-Carboxytetrahydroquinolines. Conformational and Stereochemical Requirements for Antagonism of the Glycine Site on the NMDA Receptor. *J. Med. Chem.* **1992**, *35*, 1942−1953.
(32) In a recent report, we demonstrated receptor tolerance to nonplanarity in the size-limited hydrophobic region for the HBAD series: Guzikowski, A. P.; Hawkinson, J.; Weber, E.; Keana, J. F. W. 6,7,8,9-Tetrahydro-3-hydroxy-1*H*-1-benzazepine-2,5-diones Via a Diels-Alder Reaction: Antagonists with a Non-Planar Hydrophobic Region for NMDA Receptor Glycine Sites. *Bioorg. Med. Chem. Lett.* **1995**, *5*, 2747−2748.
(33) The preparation of 4-aryl derivatives of **6** for use as antagonists at NMDA receptor glycine sites has been described. However, no direct comparison was made between the binding affinity of **6** and the binding affinities of the newly prepared compounds. Jackson, P. F.; Davenport, T. W.; Garcia, L.; McKinney, J. A.; Melville, M. G.; Harris, G. G.; Chapdelaine, M. J.; Damewood, J. R.; Pullan, L. M.; Goldstein, J. M. Synthesis and Biological Activity of a Series of 4-Aryl Substituted Benz[b]azepines: Antagonists at the Strychnine-Insensitive Glycine Site. *Bioorg. Med. Chem. Lett.* **1995**, *5*, 3097−3100.
(34) Such HBAD methyl ethers are reported to be neuroprotective in a gerbil ischemia model. It is hypothesized that such ethers act as prodrugs for the active HBADs; see ref 7.
(35) Randle, J. C. R.; Guet, T.; Bobichon, C.; Moreau, C.; Curutchet, P.; Lambolez, B.; Prado De Carvalho, L.; Cordi, A.; Lepagnol, J. M. Quinoxaline Derivatives: Structure-Activity Relationships and Physiological Implications of Inhibition of *N*-Methyl-D-Aspartate and Non-*N*-Methyl-D-Aspartate Receptor-Mediated Currents and Synaptic Potentials. *Mol. Pharmacol.* **1992**, *41*, 337−345.
(36) Gray, N. M.; Dappen, M. S.; Cheng, B. K.; Cordi, A. A.; Biesterfeldt, J. P.; Hood, W. F.; Monahan, J. B. Novel Indole-2-carboxylates as Ligands for the Strychnine-Insensitive *N*-Methyl-D-Aspartate-Linked Glycine Receptor. *J. Med. Chem.* **1991**, *34*, 1283−1292.
(37) Ilyin, V. I.; Whittenmore, E. R.; Tran, M.; Shen, K.-Z.; Cai, S. X.; Kher, S. M.; Keana, J. F. W.; Weber, E.; Woodward, R. M. Pharmacology of Acea-1416: A Potent Systemically Active *N*-Methyl-D-Aspartate Receptor Glycine Site Antagonist. *Eur. J. Pharmacol.*, in press.
(38) Huettner, J. E.; Baughman, R. W. Primary Culture of Identified Neurons from the Visual Cortex of Postnatal Rats. *J. Neurosci.* **1986**, *6*, 3044−3060.

JM960479Z